

Preparation and characterization of polyethylene (PE)/clay nanocomposites by *in situ* polymerization with vanadium-based intercalation catalyst

Liqiang Cui and Seong Ihl Woo (✉)

Department of Chemical and Biomolecular Engineering & Center for Ultramicrochemical Process Systems (CUPS), Korea Advanced Institute of Science and Technology, 373-1 Guseong-dong, Yuseong-gu, Daejeon, 305-701 Republic of Korea
E-mail: siwoo@kaist.ac.kr; Fax: +82-42-869-8890

Received: 28 November 2007 / Revised version: 22 July 2008 / Accepted: 25 July 2008
Published online: 20 August 2008 – © Springer-Verlag 2008

Summary

Complete exfoliation of clay during vanadium-based Zigler-Natta polymerization of ethylene has been successfully carried out by using clay and MgCl₂ hybrid supports. MgCl₂ offers catalyst loading sites, and the vanadium catalyst is avoided directly anchoring in the surface of the clay, so intercalation catalyst clay/MgCl₂/VOCl₃ displays high activity for ethylene polymerization. Exfoliated PE/clay nanocomposites are confirmed by X-ray diffraction (XRD), and transmission electron microscopy (TEM). Strong interaction between the dispersed clay particles and the polymer matrices provides good thermal and mechanical properties. Compared with pure PE, all these nanocomposites show enhancement of the melting temperature (T_m) and the thermal decomposition temperatures. Additionally, the incorporation of clay into the PE matrix significantly improves the mechanical properties of these nanocomposites. The increased tensile strength has been observed in the range of 3.4 to 7.9 MPa. The tensile moduli of the PE/clay nanocomposite are 23.4%–45.3% higher than that of the pure PE.

Introduction

The expansion of industrial and economic activities demands new, low-cost materials to meet increasing stringent conditions. Polymer-layered silicate nanocomposites are new class of organic polymer materials, which serve as novel composite materials [1,2]. Clay with a few weight percentages in the reinforced polymer nanocomposites strongly influences polymer properties. Significant improvements have been made in physical and mechanical properties, such as higher heat distortion temperatures, an enhanced flame resistance, an increased modulus, better barrier properties, a reduced thermal expansion coefficient, and altered electronic and improved optical properties [1–4]. Polyethylene (PE) is one of the most widely used classes of polymers with relative low cost, but its mechanical properties are poor. Therefore the preparation of the PE/clay nanocomposites has attracted a large of attention. In general, three methods *in situ* polymerization [5–12], melt intercalation [13–21] and solution blending [22–24] are mainly used to prepare polymer /clay nanocomposites. Among

the three methods, the *in situ* polymerization has been proved to be a promising method for preparing fully exfoliated polyolefin/clay nanocomposites [25].

More recently, many Zigler-Natta catalysts have been used to synthesize polyolefin nanocomposites. Typical Zigler-Natta catalyst has the advantage of using industrial catalysts, the most cost-effective among coordination catalysts. Rong et al. [26] used $TiCl_4$ catalyst supported on the surface of nanoscale crystal of palygorskite to initiate ethylene polymerization on the surface of the fiber. Kwak et al. [27] reported that $TiCl_4$ first reacted with modified montmorillonite (MMT-OH) at 30°C and then the cocatalyst Et_3Al was introduced to activate $TiCl_4$. Complete exfoliation of MMT during Ti-based Ziegler-Natta polymerization has been successfully carried out, but the clay dispersion is not uniform. Yang et al. [28] used MMT/ $MgCl_2/TiCl_4/AlEt_3$ catalyst system to synthesize PE nanocomposites. The nanoscale dispersion of MMT layer in the PE matrix was characterized. The tensile strength was significantly improved compared to that of virgin PE.

It is well known that vanadium-based support catalysts have relatively high initial activity for ethylene polymerization [29]. In the present study, we have developed an *in situ* exfoliation method during ethylene polymerization by fixing a V-based catalyst at surface of $MgCl_2$ and montmorillonite. Intercalation MMT/ $MgCl_2\cdot nEtOH/VOCl_3$ (V-MMT) has been synthesized and the intercalation structure is confirmed by XRD. Furthermore, this intercalation catalyst is initially used to prepare the PE/clay nanocomposites. The structure and properties of the prepared PE/clay nanocomposites are also investigated.

Experimental

Materials

Sodium montmorillonite (Kunipia F, Cation Exchange Capacity (CEC) 119 meq/100 g, surface area: 750 m²/g) supplied by Kunimine Co. was used as received. Vanadium (V) oxytrichloride ($VOCl_3$, 99%), Magnesium chloride (98%) and $Al(i-Bu)_3$ purchased from Aldrich were used without further purification. Anhydrous *n*-heptane, dichloromethane and ethanol were received from Aldrich. Decalin (99%) was supplied by Kanto Chemical Co. Polymerization purity grade ethylene, which was donated by Daerim Petroleum Company, was used after passing the oxy trap and molecular sieve trap to remove oxygen and water.

Intercalation of montmorillonite (MMT) with $MgCl_2$

Intercalation of $MgCl_2$ in the layers of the MMT was prepared as follows. Typically, 5.0 g $MgCl_2$ was dissolved in 50 mL anhydrous ethanol at 60°C for 4 h. 10 g MMT was dispersed in 50 mL ethanol. Following this, $MgCl_2$ ethanol solution was added with a dropper into the clay suspension under nitrogen and consequent reaction for 48 h at 60°C. The suspension was then washed several times with anhydrous ethanol in order to eliminate the excessive $MgCl_2$. The precipitate was then vacuum-dried at 70°C for 12 h to produce MMT/ $MgCl_2\cdot nEtOH$ support.

Immobilization of $VOCl_3$ catalyst

MMT/ $MgCl_2\cdot nEtOH$ (2.0 g) was dispersed in 30 mL anhydrous CH_2Cl_2 under stirring. 10 mL $VOCl_3$ (0.10 mol) was added with a dropper and stirred at room temperature.

The mixture was refluxed for 48 h under a nitrogen atmosphere, followed by washing with 5×30 mL of dry CH_2Cl_2 . After drying under a vacuum for 12 h at 60°C , intercalated catalyst MMT/ $\text{MgCl}_2\cdot n\text{EtOH}/\text{VOCl}_3$ (V-MMT) was obtained. The composition of catalyst was analyzed by inductively coupled plasma-atomic emission spectroscopy (ICP-AES) to be V, 0.26 wt% and Mg, 2.79 wt%.

Preparation of the PE/clay nanocomposites

The ethylene polymerization was carried out in the 250 mL glass flask with a magnetic stirrer. 100 mL *n*-heptane, desired amounts of V-MMT and $\text{Al}(i\text{-Bu})_3$ with various molar ratio were introduced into the flask. The polymerization was started as the ethylene was introduced into the reactor. The polymerization was carried out at room temperature with supplying ethylene under a pressure of 1.2 atm to keep the polymerization proceeding for a designated period of time. The reaction was terminated by adding acidified methanol solution. The polymer was obtained by precipitation and dried at 60°C in vacuum for 12 h.

Characterization

X-ray diffraction (XRD) patterns were obtained by using a Rigaku X-ray diffractometer (Rigaku Co.) with $\text{Cu-K}\alpha$ radiation ($\lambda = 0.15406$ nm) at room temperature. The XRD patterns were recorded in the range $1.2\text{--}10^\circ$ at a rate of $1^\circ/\text{min}$. Fourier transform infrared analysis (FT-IR) spectra were obtained in the range of $4000\text{--}400\text{ cm}^{-1}$ at a resolution of 4.0 cm^{-1} using a MAGNA-IR 560 (Welltech Enterprises, Inc.) at room temperature. The KBr pellet method was used in the measurement. Transmission electron microscope (Philips CM20) operated at an acceleration voltage of 120 KV was used to observe the dispersibility of the clay in the hybrids. Ultrathin sections of 70-80 nm in thickness were prepared by an ultramicrotome Leica EM FCS. The thermal decomposition temperature of pure PE and PE/clay nanocomposites were investigated by thermogravimetric analysis (TGA) with a TGA-Q500 thermoanalyzer instrument (TA Instrument). In each case, the specimens were heated from 50 to 700°C at the rate of $10^\circ\text{C}/\text{min}$ under nitrogen flow. DSC was performed on a TA2000 differential scanning calorimeter (TA Instrument) at a heating or cooling rate of $10^\circ\text{C}/\text{min}$ in a nitrogen atmosphere. The temperature range was from 30 to 160°C , for two continuous scanning cycles. The data set obtained from the second scanning was accepted. The tensile test was carried out according to ASTM D 882 using an Instron 5583 of INSTRON Co. at a crosshead speed of 10 mm/min.

Results and discussion

Structure and properties of V-MMT

The key step for producing *in situ* polymerized nanocomposites is to fix the catalyst into the silicate layers of the clay without sacrificing the high catalytic activities of the catalyst. MgCl_2 is an essential component in typical highly active Zigler-Natta catalysts. It was firstly deposited on the internal surfaces of the clay and the hybrid MMT/ $\text{MgCl}_2\cdot n\text{EtOH}$ was used as a support for vanadium catalyst. Figure 1 displays the XRD patterns of pristine MMT (a), MMT/ $\text{MgCl}_2\cdot n\text{EtOH}$ (b) and V-MMT (c). The pristine MMT provides a diffraction pattern with (001) reflection peak at $2\theta = 7.5^\circ$

corresponding to a distance of 11.9 Å, while the MMT/MgCl₂·nEtOH presents a $d_{(001)}$ diffraction peak at $2\theta = 6.3^\circ$ ($d_{(001)} = 13.9$ Å) resulting from the formation of MgCl₂ intercalated into layers of clay [28]. When catalyst VOCl₃ immobilized on the support of MMT/MgCl₂·nEtOH, V-MMT displays its characteristic peaks at $2\theta = 5.8^\circ$ ($d_{(001)} = 15.1$ Å). This indicates that two-steps intercalations of MgCl₂ and VOCl₃ resulted in the layer distances of the clay increasing from 11.9 Å to 15.1 Å.

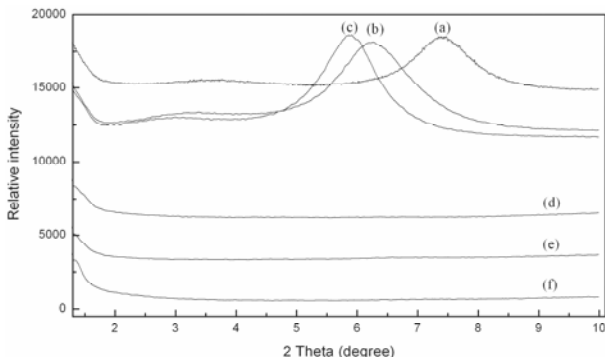


Figure 1. WAXD patterns of (a) pristine MMT (Kunipia F) (b) MMT/MgCl₂·nEtOH (c) MMT/MgCl₂·nEtOH/VOCl₃ (d)-(f) PE/clay nanocomposites with the clay loading 1.61 wt%, 2.43 wt% and 3.76 wt%

This V-MMT compound acts as an effective catalyst for ethylene polymerization, as indicated in Table 1. Polyethylene with different clay loading was synthesized by varying the polymerization time and the amount of catalysts. V-MMT shows fairly good activity up to 76.0 PE_{kg}/V_{mol}·h·atm compared with the homogeneous vanadium catalyst, behaving as the high active MgCl₂-supported Zigler-Natta catalysts. The clay contents in the final polymer were calculated using the initial clay loading and the polymer yields.

Properties of PE/MMT composites

Extraction of polyethylene chains from the hybrid PE/clay composites was carried out using reflux solvent (decalin) in a Soxhlet extractor for 24 h. Results show that only part of the PE could be extracted and the extracted amount of the PE decreases with the increase of the clay loading in the PE matrix. When clay dispersed in PE matrix, the clay layers can stiff the PE chains and impede the movements of the PE chains, especially when the particular network is formed [30]. The thermal stabilities of the PE/clay nanocomposites and pure PE studied by TGA analysis are also shown in Table 1. The temperature for 5% weight loss is defined as the thermal decomposition temperature (T_d) [31]. The PE/clay composites show higher thermal decomposition temperature (T_d Run No.2-4 = 388, 403, 426°C) than that of pure PE ($T_d = 367^\circ\text{C}$). As compared to 10% weight loss of PE/clay composites and pure PE, the thermal decomposition temperatures show 3-79°C higher with increasing clay contents in PE matrix. The effect of the clay on the thermal stability of the nanocomposite is more pronounced and the thermal decomposition temperature of the nanocomposite is shifted to higher temperature with increasing clay contents in experimental range. The

melting temperature (T_m) of the final hybrid PE/clay composites is measured using DSC. As expected, all of the PE/clay nanocomposites exhibit a higher endothermic peak at around 133–134°C than that of pure PE (Run No.1 from Table 1, 130°C), as shown in Figure 2. The strong interaction between the clay and PE matrix can restrict the motion of the polymer chain, thus a higher melting temperature of the PE/clay composites is obtained from polymerizations carried out using the intercalation catalyst at the same polymerization temperature and pressure. On the other hand, the clay layers also have good barrier actions, which can improve the thermal stability of the PE/clay nanocomposites. Compared with previous report [28], the T_m of PE/clay nanocomposites prepared by TiCl_4 intercalated / $\text{MgCl}_2\text{-nButanol}$ have no evident improvement and it is almost the same as those of the virgin PE. Simon et al. [32] prepared PE/clay nanocomposites by *in situ* polymerization using (1,4-bis(2,6-diisopropylphenyl)-acenaphthenediimine) dichloro nickel (dad-NiCl₂) intercalation catalyst. PE/clay hybrid nanocomposites display very low T_m compared with our results, though they have very high clay contents in PE matrix. Parallel experiments were carried out, and the experiment results turned out to be reproducible.

Table 1. Ethylene polymerization with intercalation catalyst V-MMT

Run No.	Initial clay loading (g)	Polymerization time (h)	Activity ^a	Clay mass fraction (wt%)	Extracted in decalin (%)	T, for 5 wt% loss (°C) ^b	T, for 10 wt% loss (°C) ^b
1 ^c	0	2	2.60	0	82.7	367	419
2	0.15	12	50.7	1.61	73.4	388	422
3	0.10	24	28.0	2.43	40.4	403	444
4	0.10	12	36.2	3.76	23.4	426	498

Polymerization conditions: $\text{Al}(i\text{-Bu})_3$ as cocatalyst, $[\text{Al}]/[\text{V}] = 1000$, *n*-heptane 100 ml as solvent, room temperature, ethylene 1.2 atm.

^a PE kg/V_{mol}·h·atm

^b Determined by TGA

^c Homogeneous catalyst VOCl_3 as catalyst, $[\text{V}] = 1.05$ mmol, $[\text{Al}]/[\text{V}] = 15$, other conditions are same as other samples

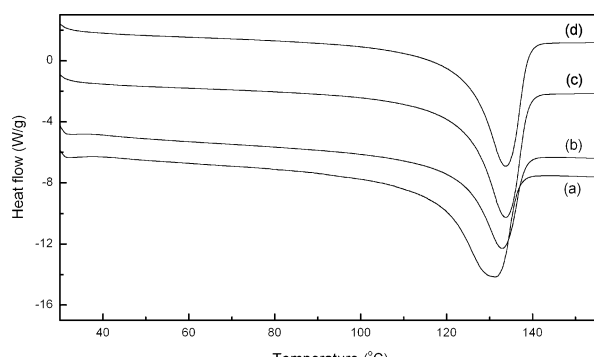


Figure 2. DSC thermograms of pure PE (curve a), PE-clay 1.61 wt% (curve b), PE-clay 2.43 wt% (curve c), and PE-clay 3.76 wt% (curve d)

Nanostructure of PE/MMT composites

Figure 1 (d, e, f) shows XRD pattern of the PE/clay nanocomposites with different clay contents. No diffraction peak is observed for the PE/clay nanocomposites in the 1.2-10° angle regions, indicating lack of long-range-ordered, face to face aggregation of the clay layers in the PE matrix. The loss of a layered structure and thus the possible exfoliation of the silicate layers result from that monomer molecules can easily diffuse the layer of the clay and be initiated by intercalated vanadium catalyst. In this case, while the PE chains grow, they tend to push the silicate layers apart from each other, resulting in the ultimate exfoliation of the layered organization. The exfoliation structure of the clay in the PE matrix is further confirmed by a TEM microphotography.

The interaction between silicate layers of the clay and the polymer matrix has been studied by FT-IR characterization. The representative FT-IR spectra of the pristine Kunipia F (a), pure PE (b) and a series of decalin-extracted PE/clay nanocomposites (c-e) are shown in Figure 3. In the IR spectrum of Kunipia F, characteristic absorbance bands occur in the following assignment: OH stretching at 3632 cm⁻¹, coordination and absorbed water peak at 3430 and 1640 cm⁻¹, Si-O stretching at 1040 cm⁻¹ and Al-O stretching at 550 cm⁻¹ [9]. The characteristic vibration bands of the PE are C-H stretching at 2855 and 2950 cm⁻¹ and 1470 cm⁻¹(δ_{C-H}). In the IR spectrum of decalin-extracted PE/clay composites, the presence of both the characteristic group frequencies of PE and MMT can be found. These results show that only part of the PE can be extracted from the nanocomposites, and the rest of PE chains stay immobilized inside and/or on the layered silicates. This confirms that strong interactions exist between the nanometric silicate layers and the PE segments.

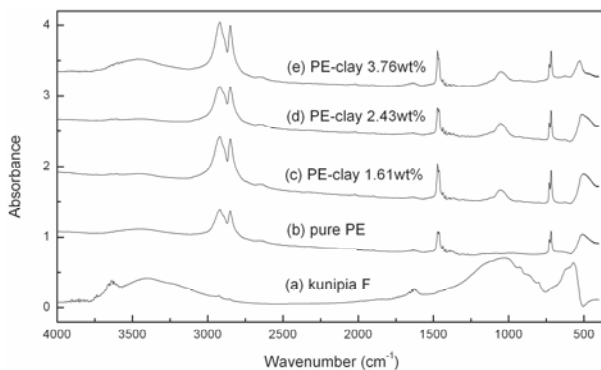


Figure 3. FT-IR spectra of pristine Kunipia F (a), pure PE (b) and decalin-extracted PE/clay nanocomposites with different clay contents (c-e)

Slides in thickness around 70-80 nm have been prepared by using an ultramicrotomy at low temperature and observed by TEM. Figure 4 shows a TEM micrograph of the PE/clay nanocomposite (Run No.4 from Table 1) having 3.76 wt% clay. The dark line represents an individual clay layer and the bright area represents the PE matrix. This shows that the clay is well dispersed in the PE matrix and the delaminated structures are only composed of an individual layer or in stacks of a few layers. Numerous single layers observed are an evidence for fully exfoliation. It can be concluded that the

stacked clay layers were exfoliated into nanometer-size layers and well dispersed in the PE matrix during the *in situ* polymerization.

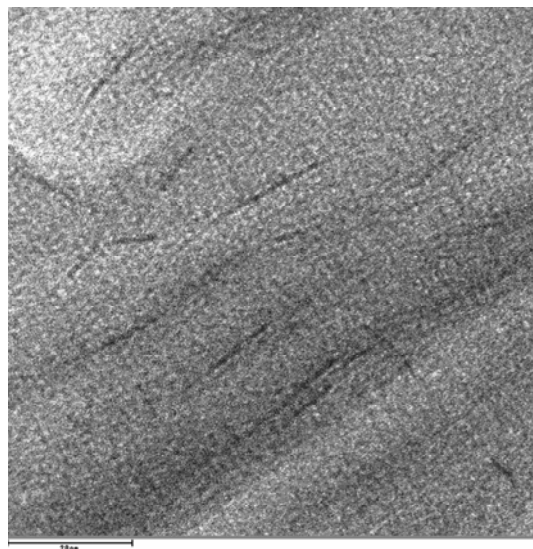


Figure 4. TEM images of the PE/clay nanocomposites (sample Run No.4, from Table 1)

Mechanical properties of PE/MMT composites

The tensile properties of PE and PE/clay composites are shown in Table 2. The tensile strength and modulus increased with contents of the clay. The elongations at break decreased when clay was introduced into PE matrix. As layered silicate is nano dispersed in PE matrix, the stress is much more efficiently transferred from the polymer matrix to the inorganic filler, resulting in a higher increase in tensile properties. Restricted segmental motions at the organic-inorganic interface and the intensified interaction between the clay layers and the chains of the polymer are the main reasons for significantly improved mechanical property of the PE/clay nanocomposites when fully exfoliated clay layers were disorderly dispersed in the polymer matrix.

Table 2. Mechanical properties of PE and PE/clay composites

Run No.	Clay contents (wt %)	Tensile strength (MPa)	Elongation at break (%)	Tensile modulus (MPa)
1	0	15.4	392.7	278.9
2	1.61	18.8	181.4	344.1
3	2.43	20.3	334.0	353.7
4	3.76	23.3	355.6	405.4

Conclusions

PE/clay nanocomposites have been successfully prepared via *in situ* polymerization of ethylene using intercalation catalyst V-MMT activated by Al(*i*-Bu)₃. V-MMT shows

much higher catalytic activity than homogeneous vanadium catalyst. Intercalation of $MgCl_2$ can not only increase the layer distance of the clay but also improve the polymerization activity of intercalated catalyst. The occurrence of exfoliation of the clay layers in PE matrix is confirmed and the interactions between the nanometric silicate layers and the polymer segments are strong. Thermal resistance of the PE/clay nanocomposites is significantly improved. The thermal decomposition temperature of the 5% and 10% weight loss of the PE/clay nanocomposites having clay 3.76 wt% is higher than that of pure PE by 60°C and 79°C. However, the T_m of the nanocomposites slightly increases. The mechanical properties of the PE/clay nanocomposites have a noticeable improvement when the clay was exfoliated and well dispersed in the PE matrix.

Acknowledgements. This work was supported by the *Center for Ultramicrochemical Process Systems* (CUPS) sponsored by KOSEF (2007) and Liqiang Cui was financially supported by the foreign student scholarship program sponsored by Korea Research Foundation.

References

1. Giannelis EP (1996) *Adv Mater* 8:29
2. Wang ZT, Pinnavaia J (1998) *Chem Mater* 10:3769
3. Bharadwaj RK (2001) *Macromolecules* 34:9189
4. Ray SS, Okamoto M (2003) *Prog Polym Sci* 28:1539
5. Heinemann J, Reichert P, Thomann R, Mulhaupt R (1999) *Macromol Rapid Commun* 20:423
6. Bergman JS, Chen H, Giannelis EP, Thomas MG, Coates GW (1999) *Chem Commun* 2179
7. Wang Q, Zhou ZY, Song LX, Xu H, Wang LJ (2004) *J Polym Sci Part A: Polym Chem* 42:38
8. Wei LM, Tang T, Huang BT (2004) *J Polym Sci Part A: Polym Chem* 42:941
9. Jeong DW, Hong DS, Cho HY, Woo SI (2003) *J Mol Catal A: Chem* 206:205
10. Xu JT, Wang Q, Fan ZQ (2005) *Eur Polym J* 41:3011
11. Ray S, Galgall G, Lele A, Sivaram S (2005) *J Polym Sci Part A: Polym Chem* 43:304
12. Huang YJ, Yang KF, Dong JY (2006) *Macromol Rapid Commun* 27:1278
13. Wang KH, Chung IJ, Jang MC, Keum JK, Song HH (2002) *Macromolecules* 43:5529
14. Gopakumar TG, Lee JA, Kontopoulou M, Patent JS (2002) *Polymer* 43:5483
15. Osman MA, Atallah A (2004) *Macromol Rapid Commun* 25:1540
16. Lee JH, Jung DS, Hong CE, Rhee KY, Advani SG (2005) *Compos Sci Technol* 65:1996
17. Osman MA, Rupp JEP (2005) *Macromol Rapid Commun* 26:880
18. Tzavalas S, Macchiarola K, Gregoriou VG (2006) *J Polym Sci Part B: Polym Phys* 44:914
19. Shah RK, Paul DR (2006) *Polymer* 47:4075
20. Truss RW, Yeow TK (2006) *J Appl Polym Sci* 100:3044
21. Lee YH, Wang KH, Park CB, Sain M (2007) *J Appl Polym Sci* 103:2129
22. Jeon HG, Jung HT, Lee SW, Hudson SD (1998) *Polym Bull* 41:107
23. Song L, Hu Y, Wang S, Chen Z, Fan W (2002) *J Mater Chem* 12:3152
24. Qiu LZ, Chen W, Qu BJ (2006) *Polymer* 47:922
25. Zanetti M, Lomakin A, Camino G (2000) *Macromol Mater Eng* 279:1
26. Rong JF, Li HQ, Jing ZH, Hong XY, Sheng M (2001) *J Appl Polym Sci* 82:1829
27. Jin YH, Park HJ, Im SS, Kwak SY, Kwak SJ (2002) *Macromol Rapid Commun* 23:135
28. Yang F, Zhang XQ, Zhao HC, Chen B, Huang BT, Feng ZL (2003) *J Appl Polym Sci* 89:3680
29. Czaja K, Bialek M (1996) *Macromol Rapid Commun* 17:253
30. Rong JF, Jing ZH, Li HQ, Sheng M (2001) *Macromol Rapid Commun* 22:329
31. Wang J, Liu ZY, Guo CY, Chen YJ, Wang D (2001) *Macromol Rapid Commun* 22:1422
32. Shin S-YA, Simon LC, Soares JBP, Scholz G (2003) *Polymer* 44:5317